# Magnetic lithography methods based on nanoindentation and ion irradiation

**J. Sort**
Departament de Física
Universitat Autònoma de Barcelona

# Collaborators

- **Departament de Física, Universitat Autònoma de Barcelona, Spain**

  A. Varea, E. Menéndez, E. Pellicer, J. F. López-Barberá, J. Fornell, A. Concustell, S. Suriñach, M. D. Baró

- **Institut de Microelectrònica de Barcelona (IMB-CNM), CSIC, Spain**

  J. Montserrat, E. Lora-Tamayo

- **Institut Català de Nanotecnologia, ICREA, Spain**

  J. Nogués

- **Others:**

  - Universidade Federal Sao Carlos, Brasil.
  - Institute of Ion Beam Physics and Materials Research, Dresden-Rossendorf, Germany.
  - Paul Scherrer Institut, Villigen PSI, Switzerland.
  - Max Planck Institute of Microstructure Physics, Halle, Germany.

# Outline

1. **Introduction**
   - Overview of magnetic recording media.
   - Origin of ferromagnetism in Fe-Al alloys.

2. **Main Goals of the Work**

3. **Experimental Details**

4. **Results and Discussion**
   - Magnetic patterning of $Fe_{60}Al_{40}$ induced by nanoindentation.
   - Magnetic patterning of $Fe_{60}Al_{40}$ induced by ion irradiation.
   - Magnetic patterning of $Fe_{67.7}B_{20}Cr_{12}Nb_{0.3}$ metallic glass induced by nanoindentation.

5. **Conclusions**

# 1. Introduction: Magnetic Recording Overview

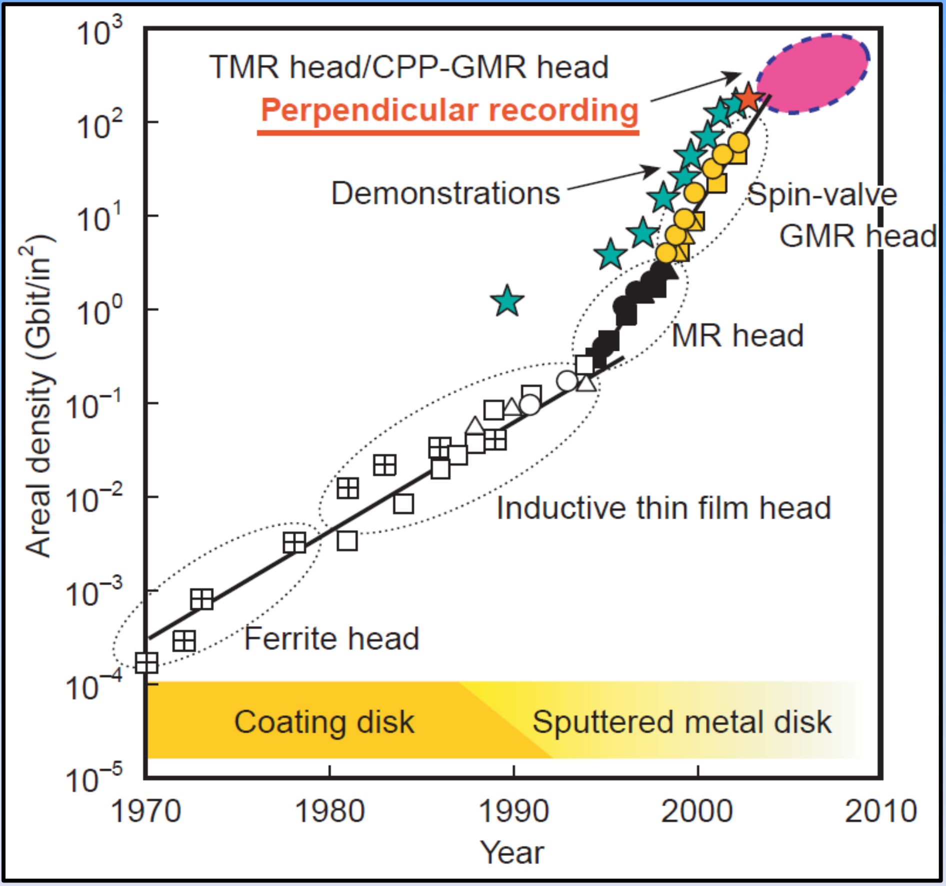


I. Kaitsu, *Fujitsu Sci. Tech. J. 42 (2006) 122.*

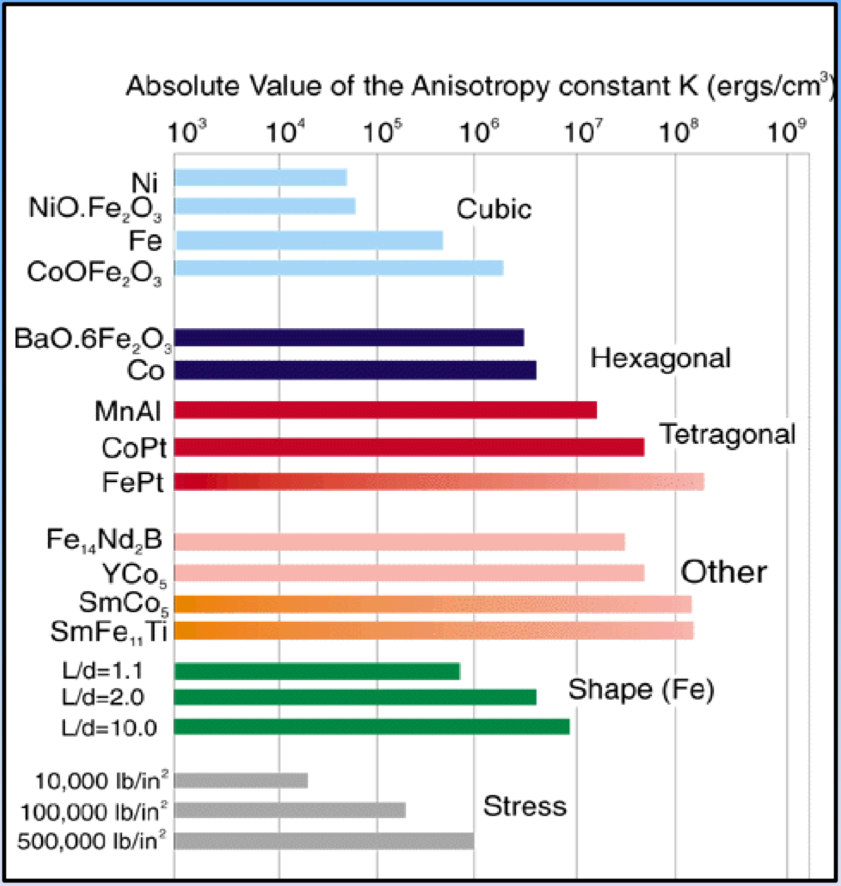


B. D. Cullity, *Introduction to Magnetic Materials*, IEEE 2009

# 1. Introduction: Ideal magnetic recording media

- Composed of submicron ferromagnetic elements arranged in a geometrically ordered manner.

- Ferromagnetic structures surrounded by a non-magnetic matrix (minimization of dipolar inter-bit interactions).

- Preservation of a smooth surface to minimize tribological problems.

- Development of fast and inexpensive lithography methods.

# 1. Introduction: Conventional e-beam lithography

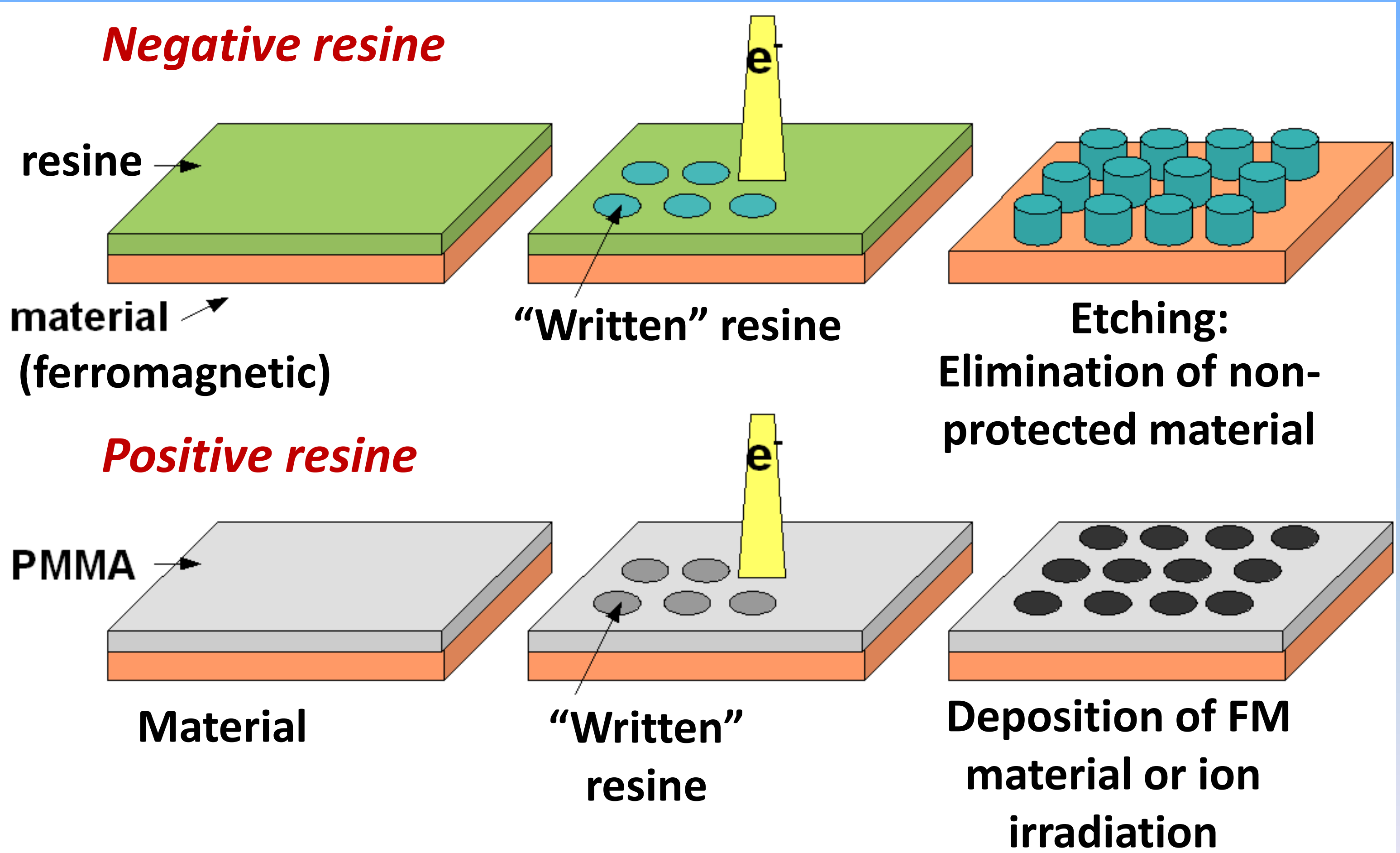

# 1. Introduction: Fe-Al system

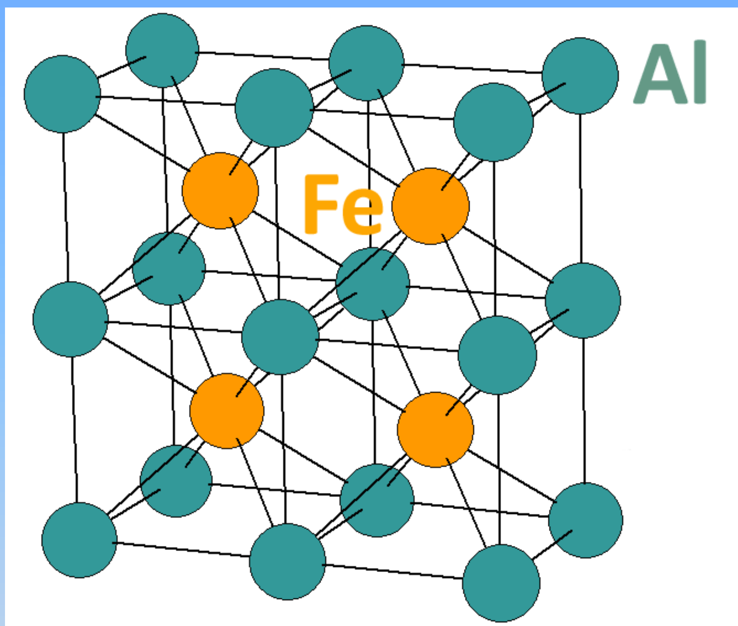


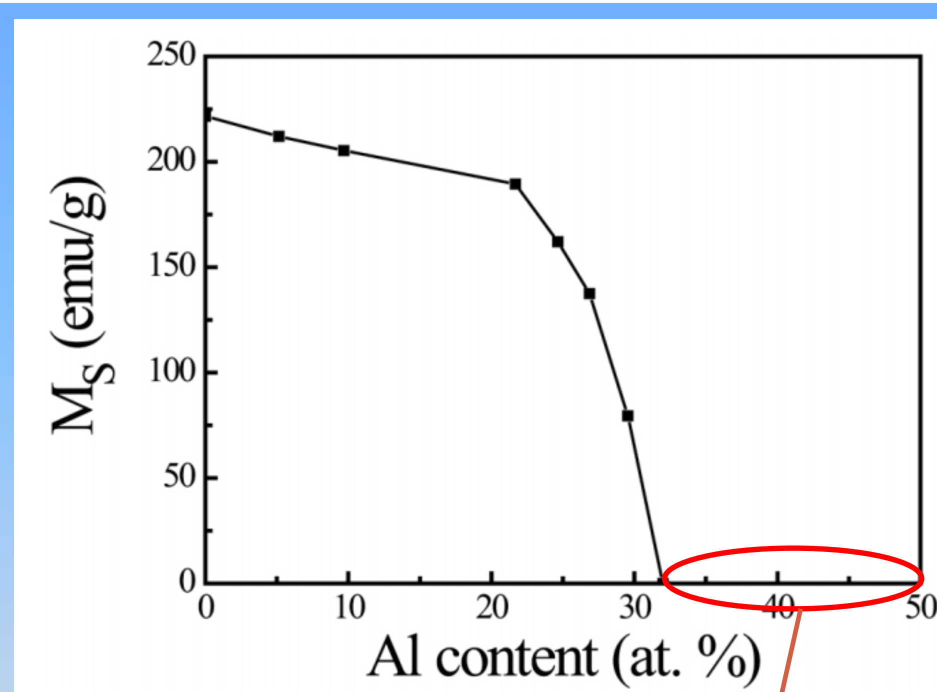


*A. Taylor, R.M. Jones, J. Phys. Chem. Solids 6 (1958) 16.*

non-ferromagnetic compositions

- For x > 32 Al at.%: Fe atoms are surrounded by Al (non-ferromagnetic behavior)

# 1. Introduction: Fe-Al system

**ORDERED STATE** → **DISORDERED STATE**

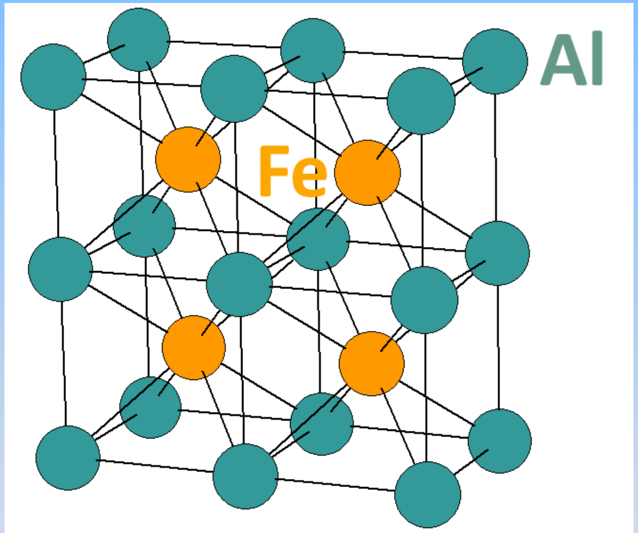


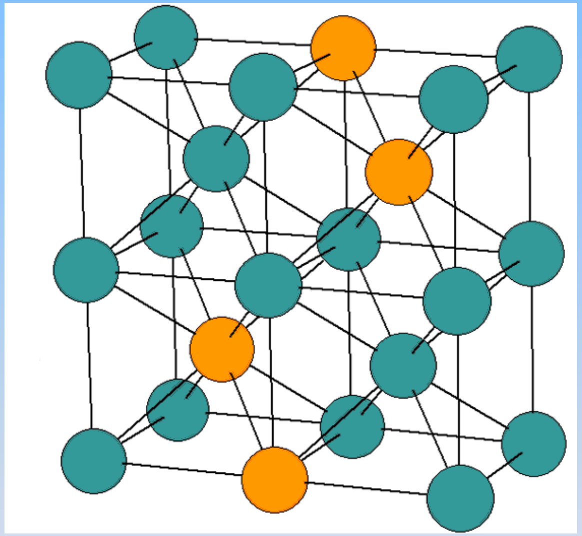

**PARAMAGNETIC-FERROMAGNETIC TRANSITION**

# 1. Introduction: Fe-Al system

**ORDERED STATE**

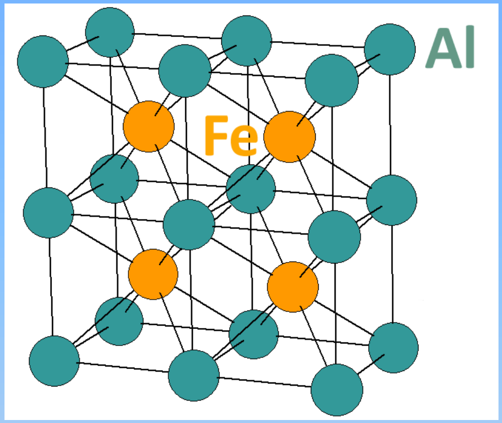


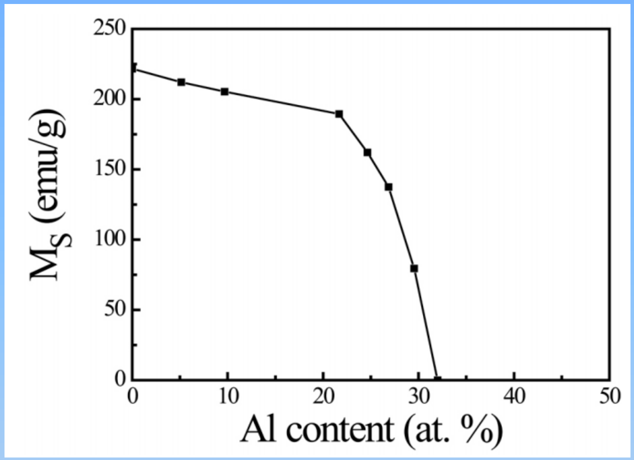


**DISORDERED STATE**

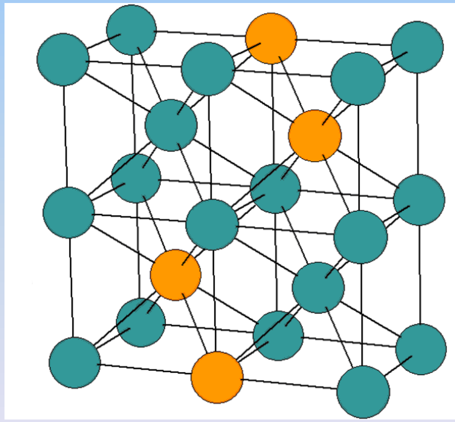

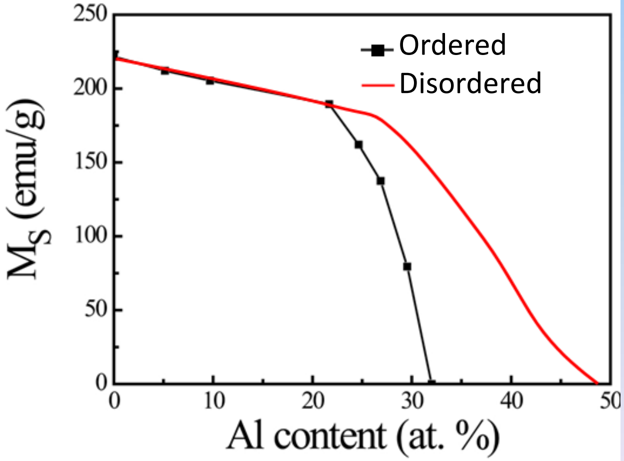

# 1. Introduction: Fe-Al system

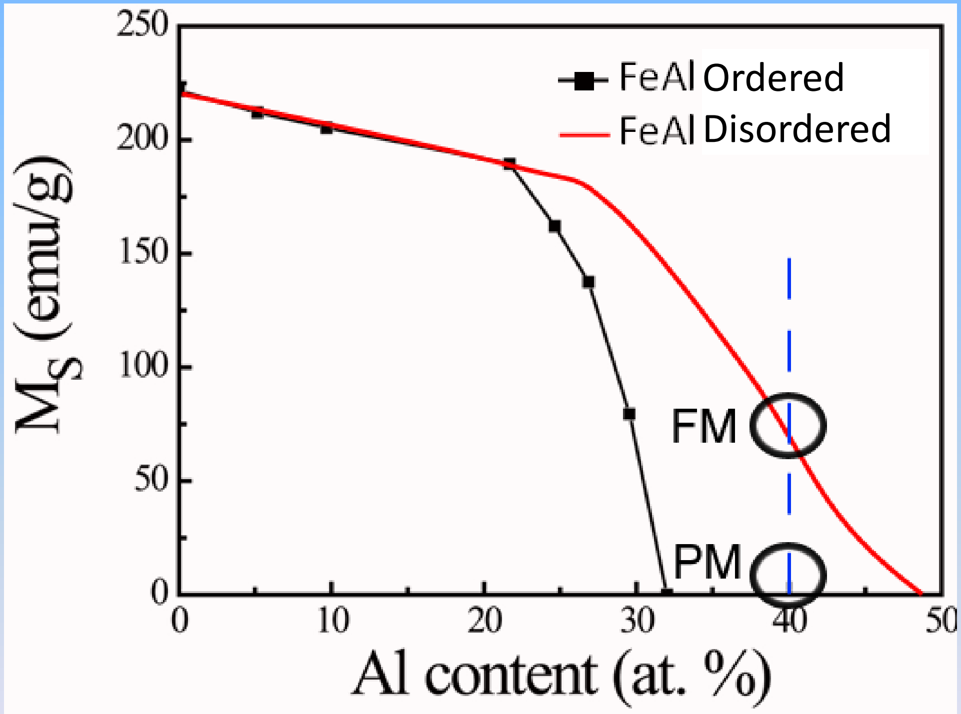

# 1. Introduction: Fe-Al system

- Two-fold origin of ferromagnetism in disordered Fe-Al:

❑ **Atomic intermixing** → changes in atomic local environment (nearest neighbors) ⇒ exchange interactions between Fe

❑ **Lattice cell expansion/reduction** → energy band modification

(changes in lattice cell parameter ($\Delta \boldsymbol{a}$)).

*E.P. Yelsukov et al., J. Magn. Magn. Mater. 115 (1992) 271*
*J. Nogués et al., Phys. Rev. B 74 (2006) 024407*

# 2. Main goals of this work

- To investigate deformation-induced ferromagnetism in $Fe_{60}Al_{40}$ alloys.
- To study the possibility of using nanoindentation and ion irradiation as magnetic patterning methods in $Fe_{60}Al_{40}$.
- To generate arrays of ferromagnetic dots surrounded by a non-magnetic matrix (minimizing interdot exchange interactions).
- To obtain perpendicular magnetic anisotropy (to increase the areal density of information). Utilization of a Fe-based metallic glass.

# 3. Experimental details

## Samples:

- **Sample 1:** Fe-40%Al-0.05% Zr-0.02%B sheet prepared by cold rolling (for simplicity, $Fe_{60}Al_{40}$).

- **Sample 2:** metallic-glass ribbon prepared by melt-spinning, with composition: $Fe_{67.7}B_{20}Cr_{12}Nb_{0.3}$

## Sample treatment:

- Mechanical polishing to mirror appearance using diamond paste.
- Eventual heat treatments (in $Fe_{60}Al_{40}$) to get rid of polishing-induced magnetic signal. Annealing at 900 K, in vacuum, for 30 min.

# 3. Experimental details

## Structure, mechanical characterization and ion irradiation

- Structural properties investigated by **X-ray diffraction, electron microscopy.**

- **Ion irradiation:** (a) Irradiation through shadow masks.
  (2 keV $He^+$, 11 keV $Ne^+$, 21 keV $Ar^+$, 35 keV $Kr^+$, 45 keV $Xe^+$)
  (b) Irradiation using focussed ion beam.

- **Nanoindentation tests**: UMIS (Fischer-Cripps Lab.)
  - Diamond pyramidal-shaped (Berkovich-type) tip.
  - Load control mode
  - Range of forces: 4 - 500 mN

# 3. Experimental details

## Topological / Magnetic Characterization (Fe-based glass)

• Scanning electron microscopy (SEM) and atomic force microscopy (AFM) imaging for **morphological investigations**.

• Local character of the induced ferromagnetism (**domain imaging**) investigated by magnetic force microscopy (MFM).

• **Hysteresis loops** recorded at room temperature using magneto-optical Kerr effect (MOKE) at 6 Hz and a laser spot radius of 5 μm.

[M $\propto \Delta$(Polarization Angle)]

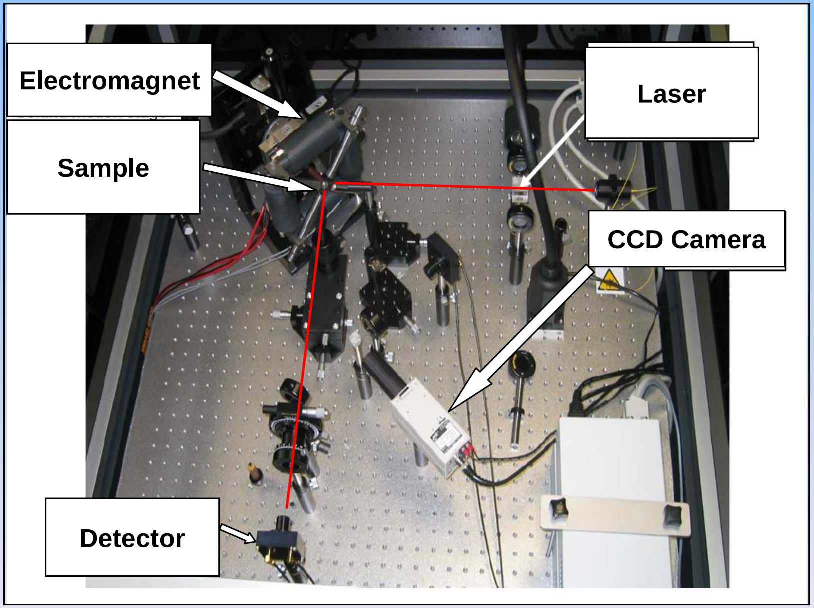


• Curie temperatures evaluated by thermo-magnetic gravimetry (TMG)

# 4. Results & Discussion: $Fe_{60}Al_{40}$

# 4. Results & Discussion: $Fe_{60}Al_{40}$

- Deformation-induced ferromagnetism by **macroscopic compression**

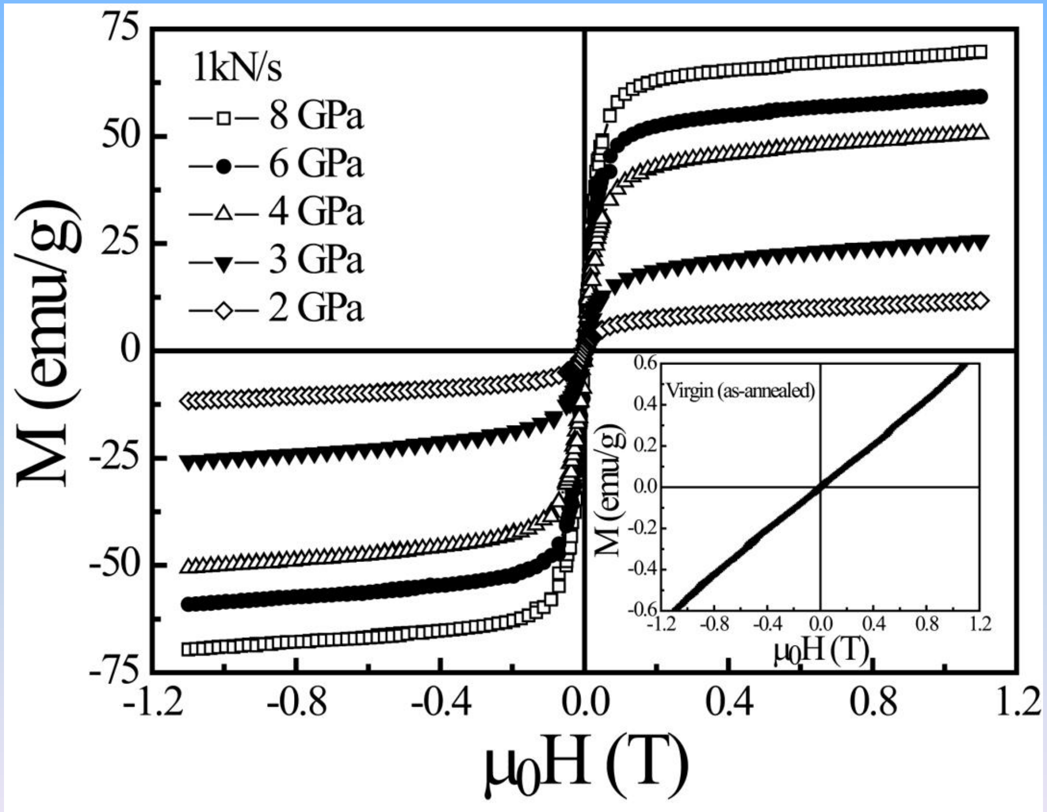


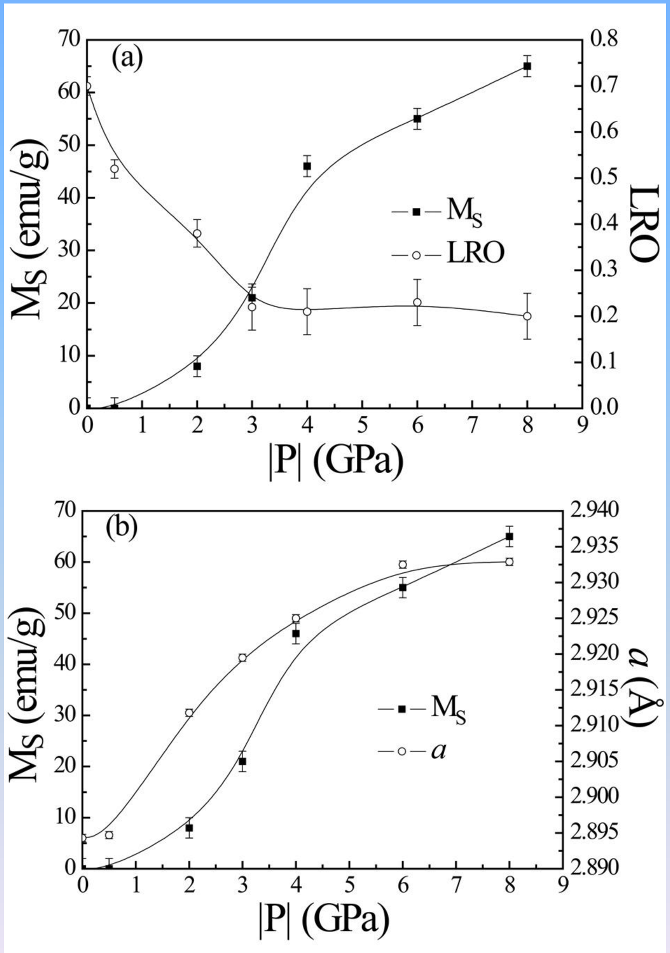

# 4. Results & Discussion: $Fe_{60}Al_{40}$

- **Nanoindentation**

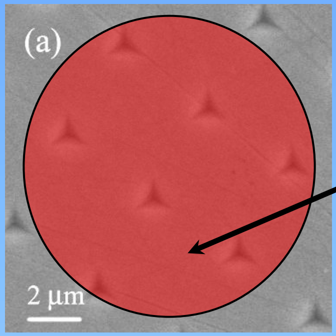


Laser spot
(measured area)

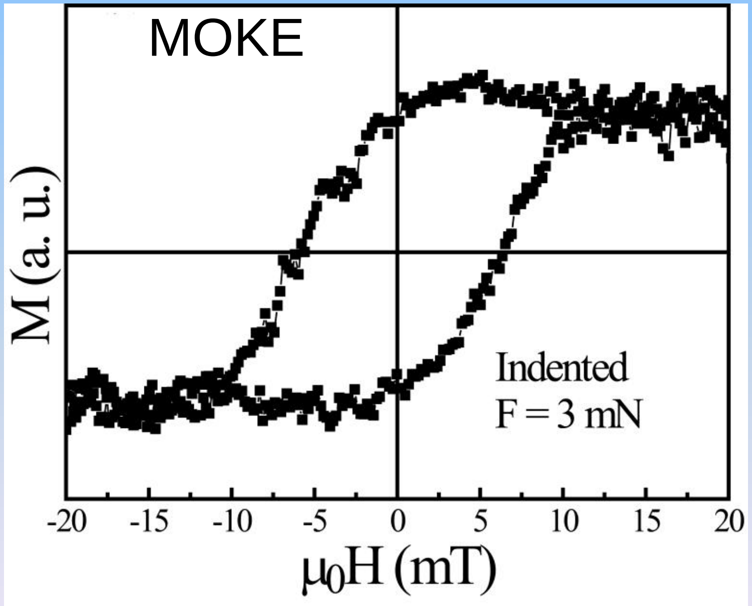


**Non-strained areas atomically ordered (paramagnetic)**

3 mN

12 mN

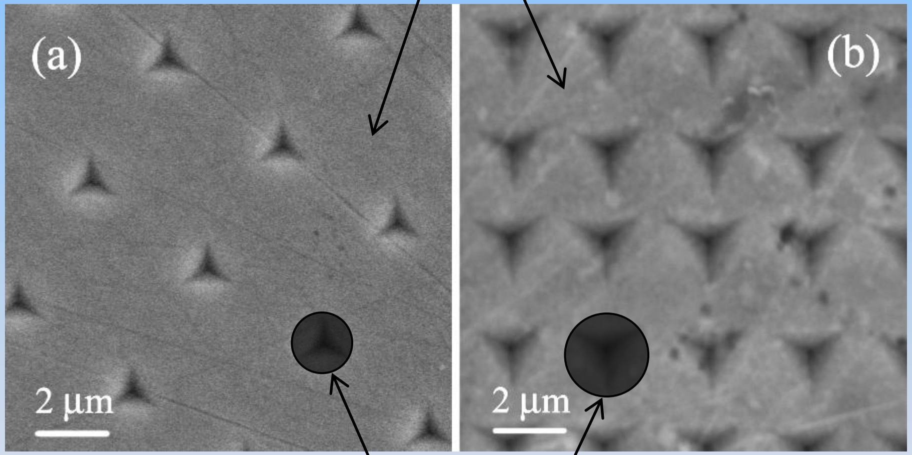


**Strained areas (ferromagnetic)**

# 4. Results & Discussion: $Fe_{60}Al_{40}$

- Deformation-induced ferromagnetism by **nanoindentation.**
- Confined magnetism, but surface topological modification!

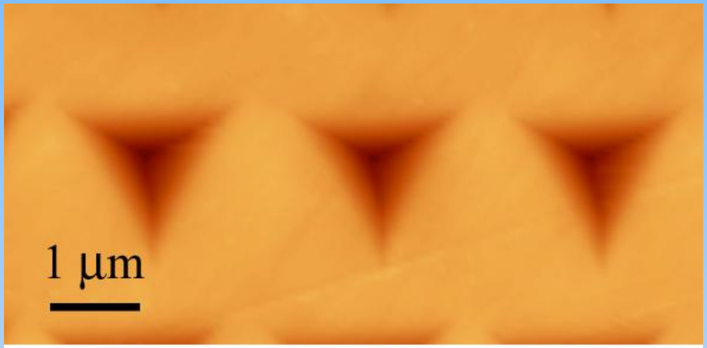


AFM

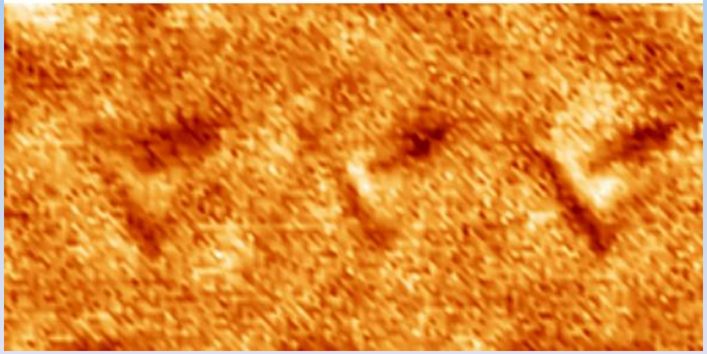

MFM

- Is it possible to obtain smaller ferromagnetic dots?
- Is it possible to obtain structures with other geometries?
- Is it possible to fabricate magnetic dots minimizing surface modification?

↓

**ION IRRADIATION?**

# 4. Results & Discussion: $Fe_{60}Al_{40}$

▪ Mechanical polishing to mirror appearance using diamond paste

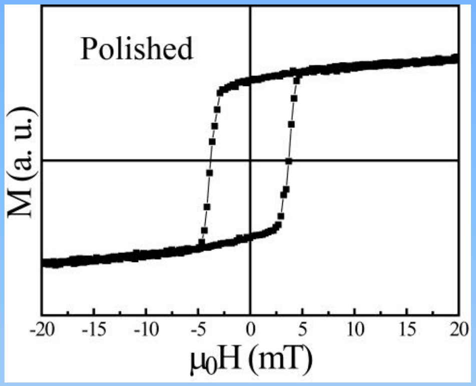


MOKE

▪ Annealing at 900 K for 30 min to remove any traces of ferromagnetism induced by the polishing

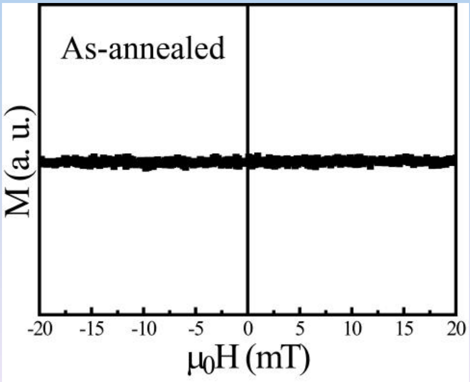


MOKE

# 4. Results & Discussion: $Fe_{60}Al_{40}$

- **Broad beam ion irradiation** ($He^+$, $Ne^+$, $Ar^+$, $Kr^+$, $Xe^+$) by a low-energy ion implanter.

- Primary energy adjusted to position the **maximum of collisional damage distribution** at a depth of **≈ 10 nm**

(**2 keV $He^+$, 11 keV $Ne^+$, 21 keV $Ar^+$, 35 keV $Kr^+$, 45 keV $Xe^+$**)

- Ion fluence varied to obtain damage, within **top 20 nm**, of **0.05 - 5 dpa** (displacements per atom)

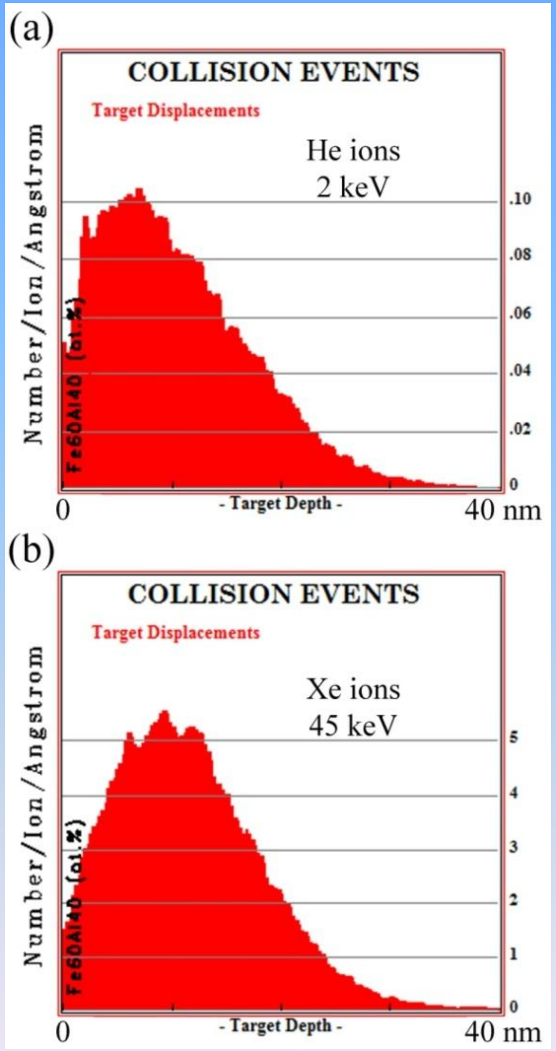


*TRIM simulations (SRIM 2006 code)*
*J.F. Ziegler, J.P. Biersack and U. Littmark, The Stopping and Range of Ions in Solids (Pergamon, New York, 1985)*

# 4. Results & Discussion: $Fe_{60}Al_{40}$

- Ion irradiation (e.g., 45 keV $Xe^{+}$)

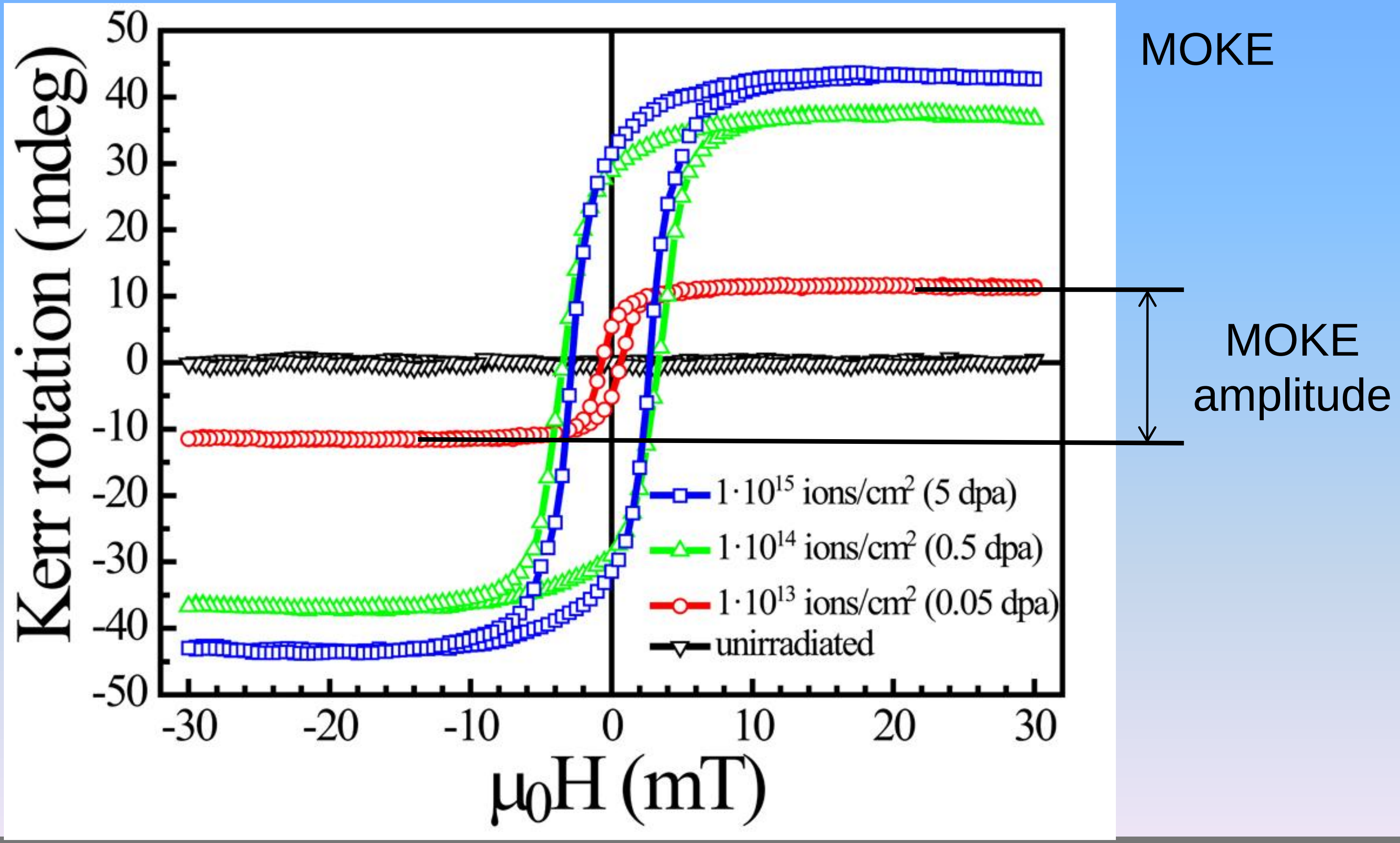

# 4. Results & Discussion: $Fe_{60}Al_{40}$

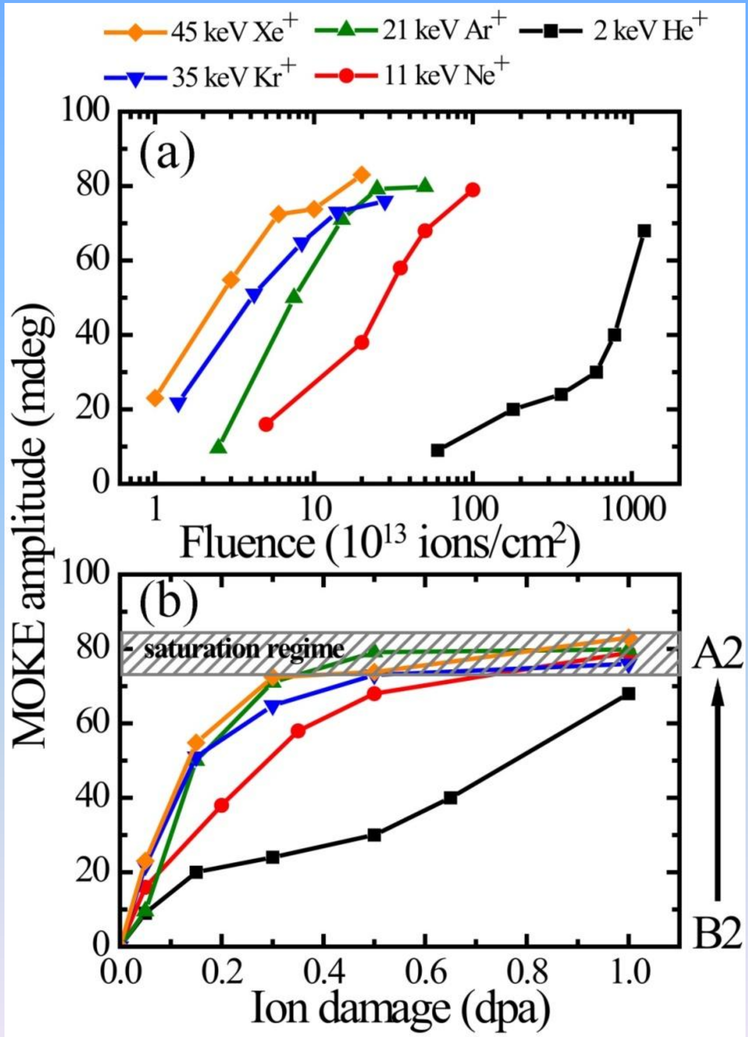


- Irradiation fluence for $He^+$ is about 3 orders of magnitude larger than for $Xe^+$.

*Universal* behavior only for heavy ions

Light ions

↓

dilute vacancy-interstitial pairs along the ion track

(all defects available for diffusion)

↓

atomic reordering

# 4. Results & Discussion: $Fe_{60}Al_{40}$

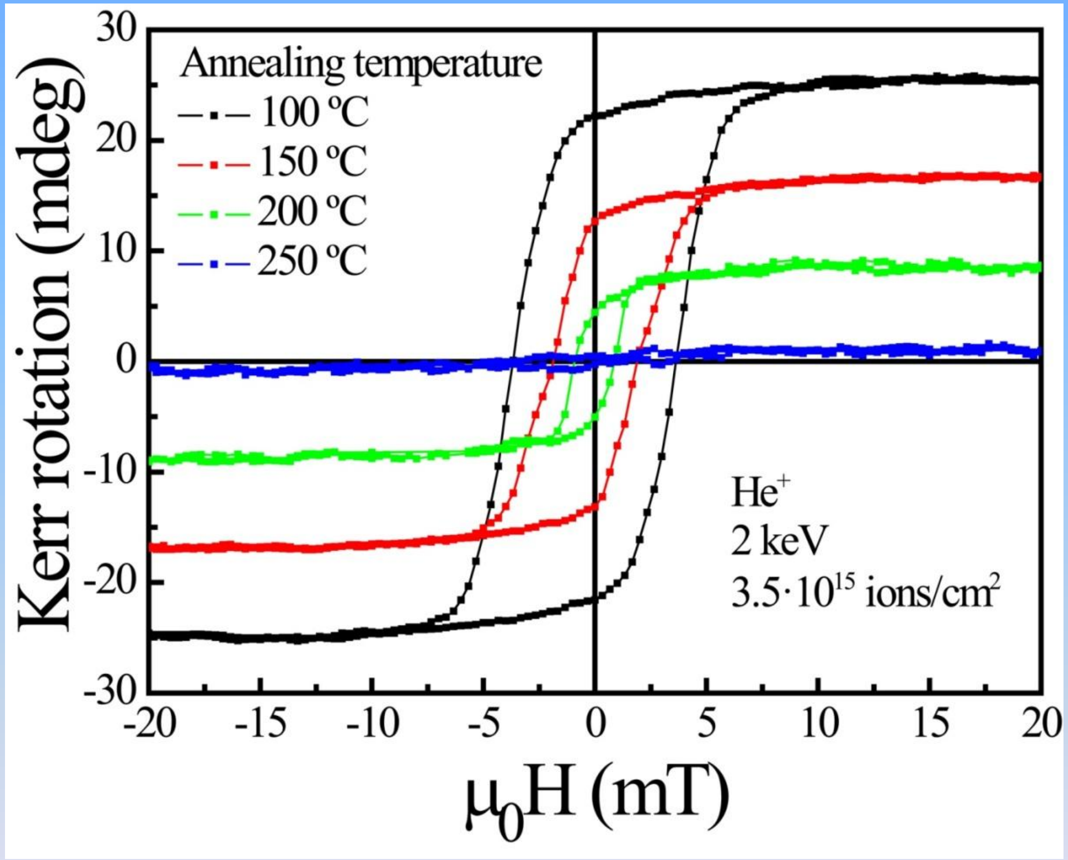


MOKE

- The induced ferromagnetism can be removed by heating (reordering process).

# 4. Results & Discussion: $Fe_{60}Al_{40}$

• **TEM grids as** shadow masks, 40 keV $Xe^+$ irradiation ($1{\cdot}10^{15}$ ions/$cm^2$)

AFM

MFM in an applied magnetic field of 40 mT

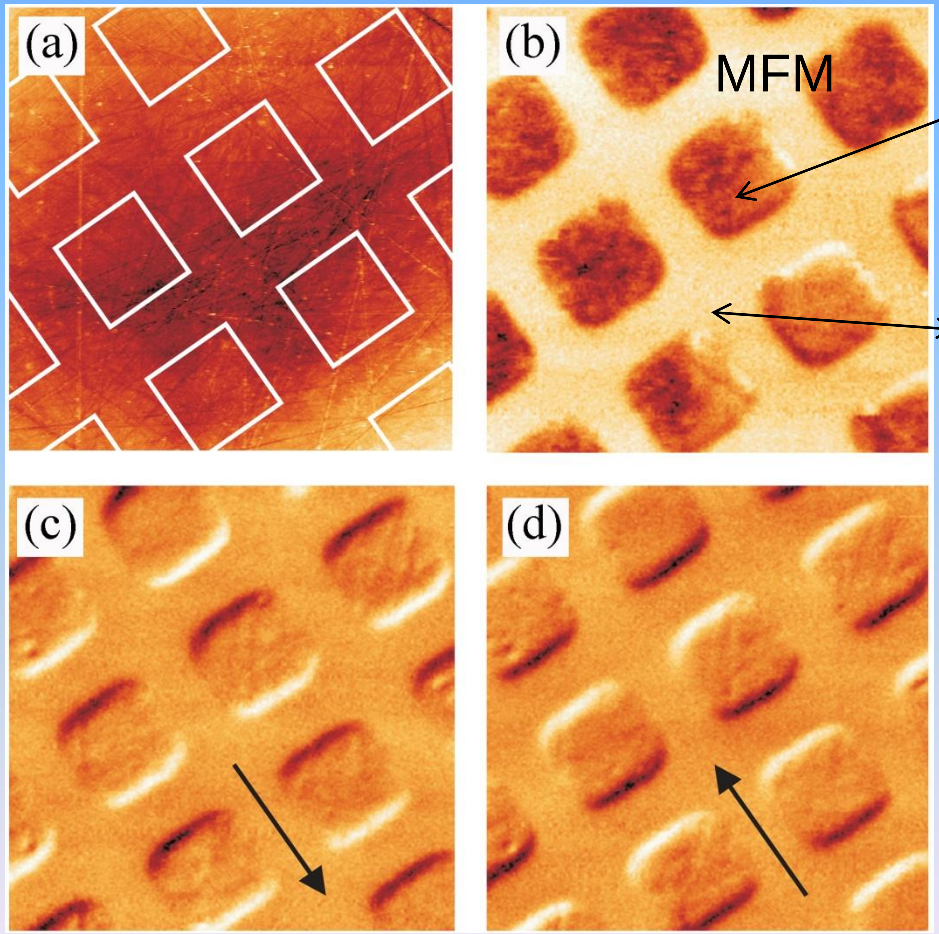


Irradiated area (ferromagnetic)

Non-irradiated area (paramagnetic)

• **Feature-less magnetic dots.**

• **Minimized surface etching.**

# 4. Results & Discussion: $Fe_{60}Al_{40}$

- **Polymethylmethacrylate** (PMMA ) shadow masks (90 nm thickness) prepared by **Electron Beam Lithography** (EBL)

40 keV $Xe^{+}$ irradiation ($1 \cdot 10^{15}$ ions/$cm^2$)

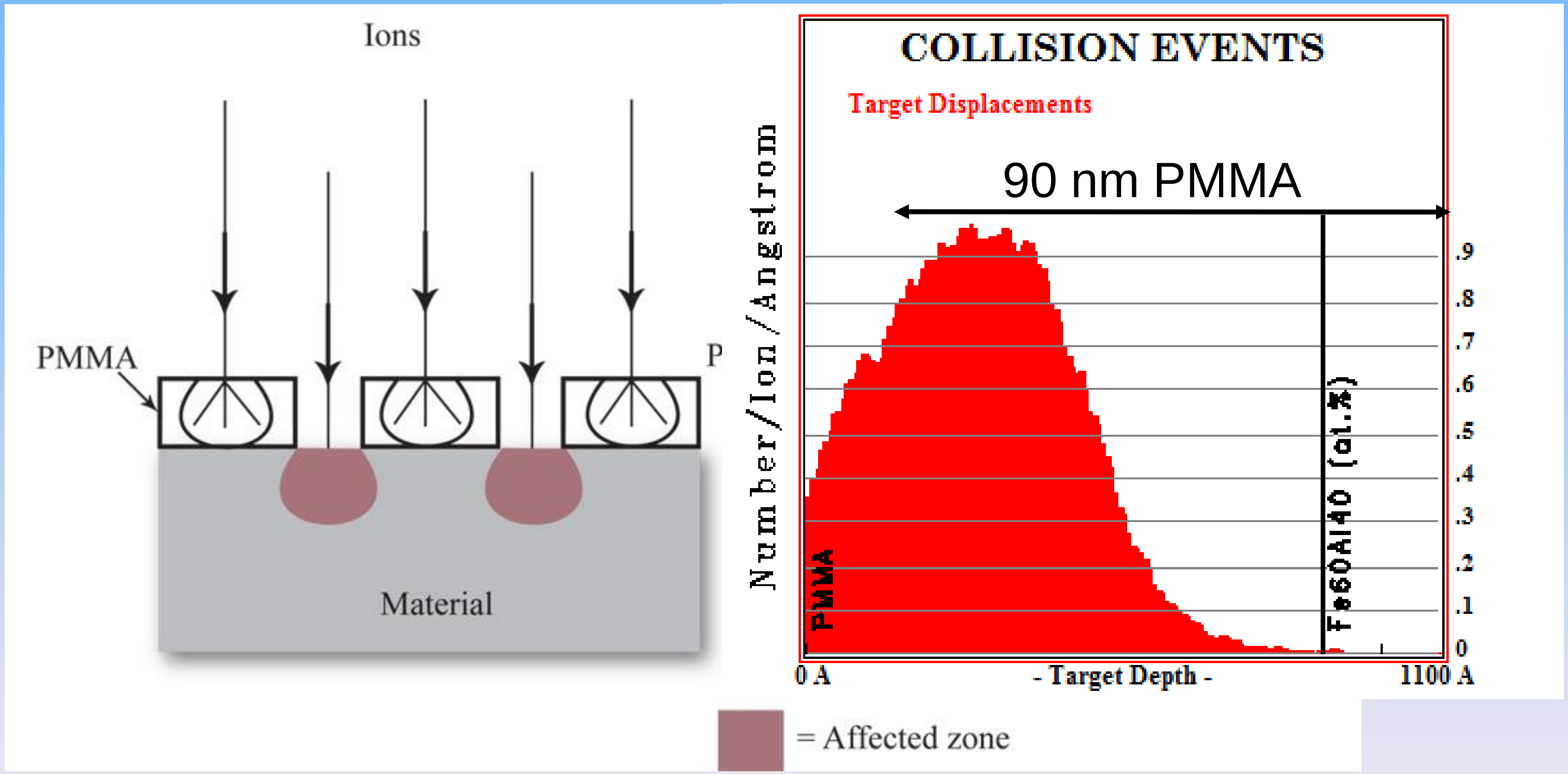

# 4. Results & Discussion: $Fe_{60}Al_{40}$

- **Ion irradiation** through EBL PMMA.

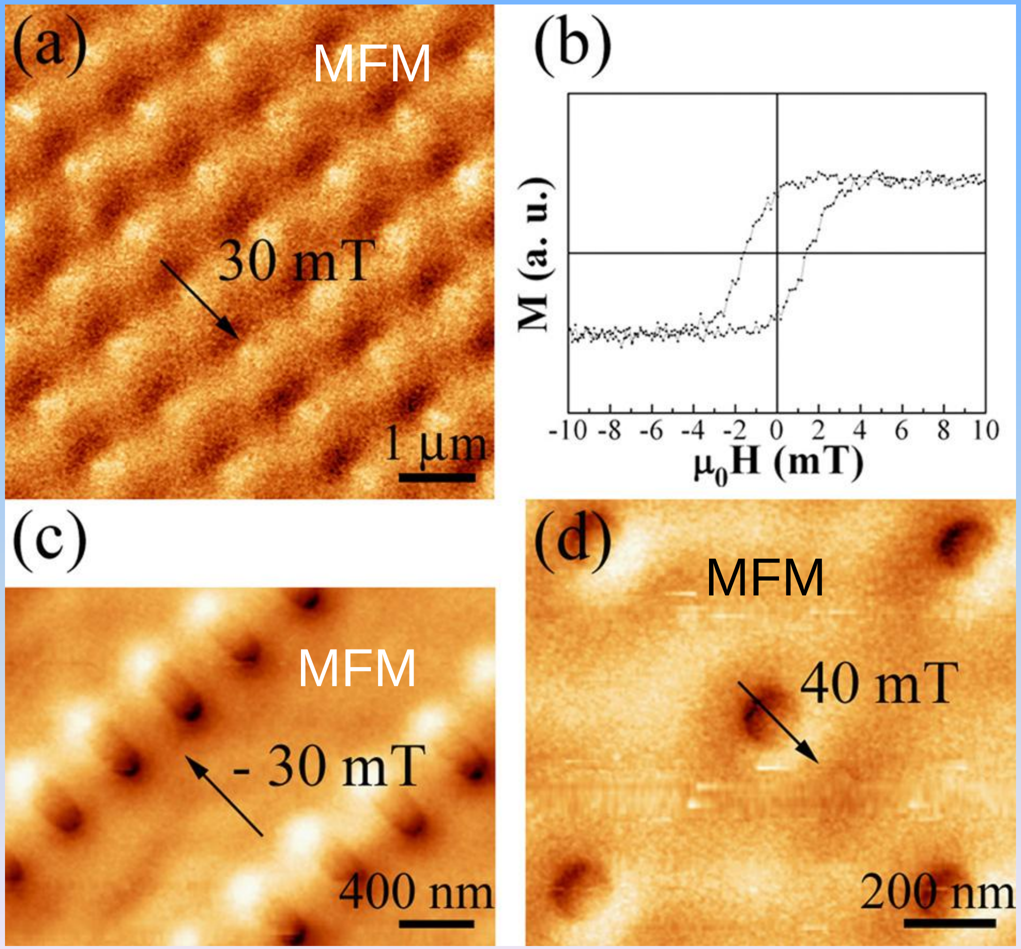


- Dots with different sizes and geometry
- Large arrays of dots (50 x 50 $\mu m^2$) are obtained at once (in-parallel process)

# 4. Results & Discussion: $Fe_{60}Al_{40}$

- **Pseudo-ordered alumina membranes** (prepared by anodization processes) placed on top of **$Fe_{60}Al_{40}$ (at.%) sheets**

(thickness ≈ 5μm, mean pore size ≈ 250-300 nm)

40 keV $Xe^+$ irradiation ($1 \cdot 10^{15}$ ions/$cm^2$)

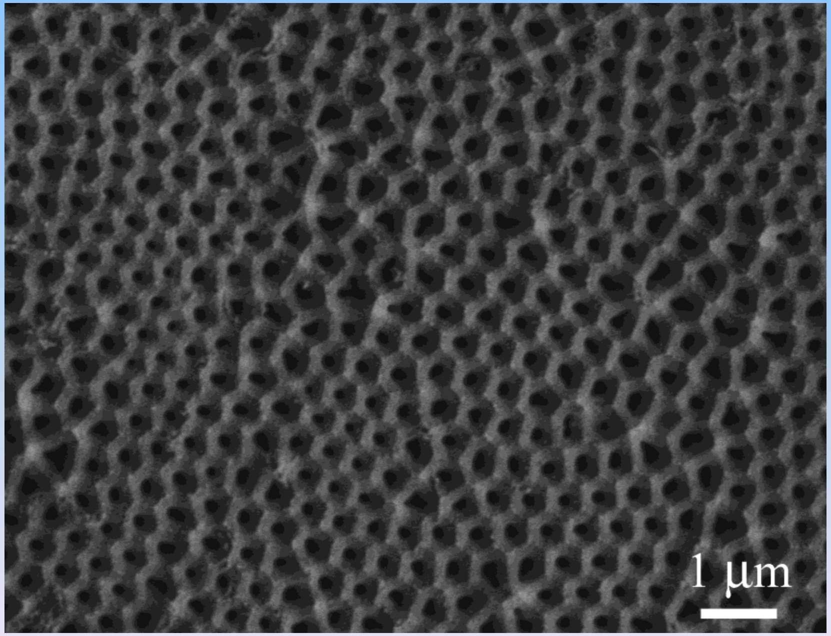


SEM

(secondary electrons)

# 4. Results & Discussion: $Fe_{60}Al_{40}$

• **Pseudo-ordered alumina membranes** (prepared by anodization processes)

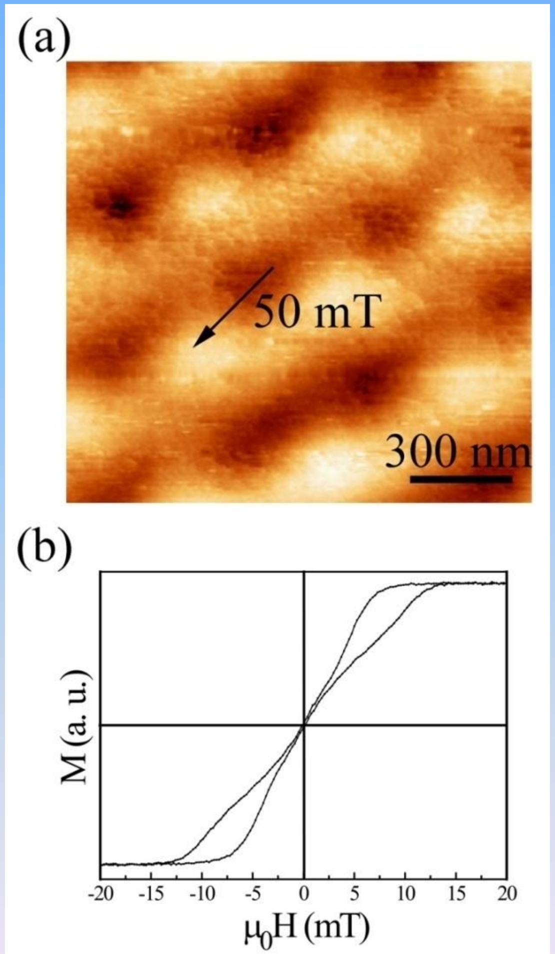


- Vortex-like loops
- Large pseudo-ordered arrays (several mm) of magnetic dots obtained at once (in-parallel process)
- Minimized surface damage

# 4. Results & Discussion: $Fe_{60}Al_{40}$

- **Focussed ion-beam irradiation** (30 keV $Ga^{+}$) ($1\text{-}5 \cdot 10^{15}$ ions/cm$^{2}$)

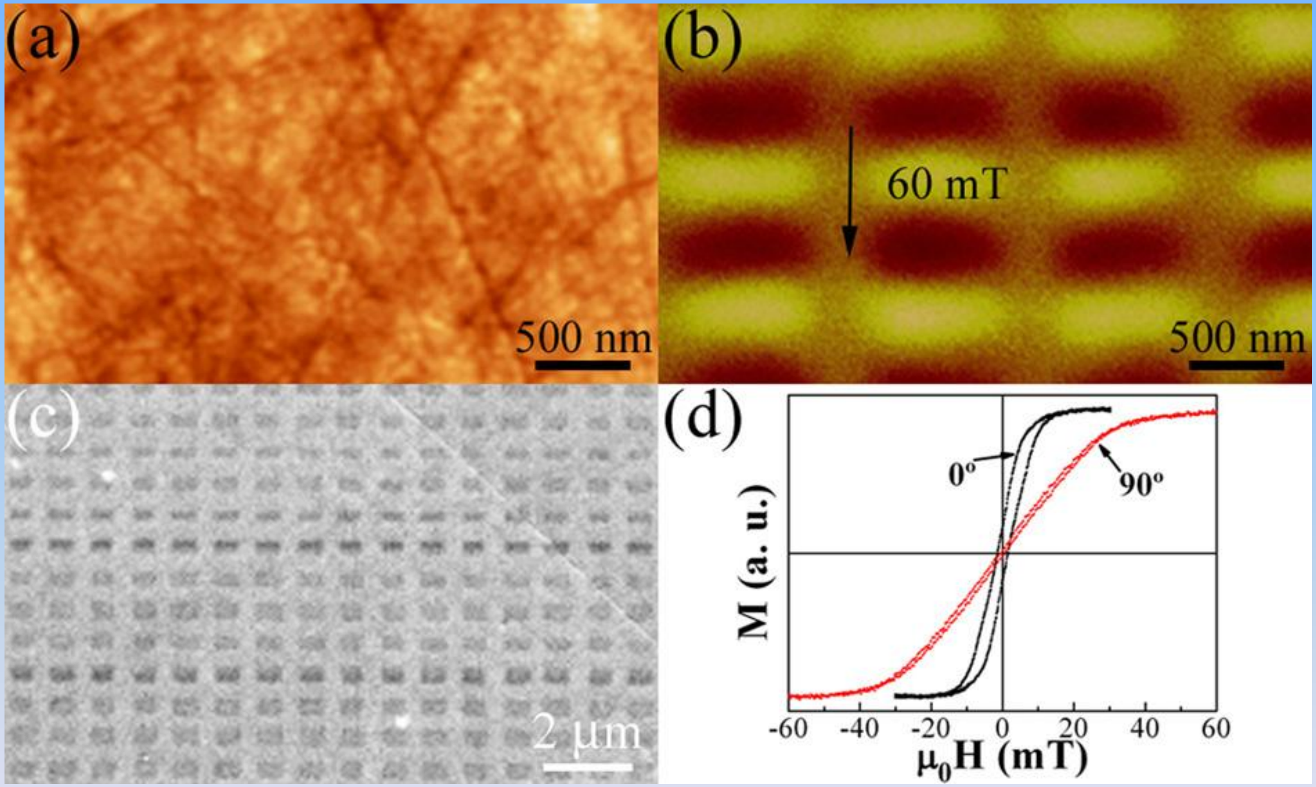


- Surface etching minimized
- Confined magnetism
- Magnetic anisotropy (dot shape)

Magnetic lithography is an in-series process

# 4. Results & Discussion: $Fe_{60}Al_{40}$

- **Focussed ion-beam irradiation** (30 keV $Ga^+$)

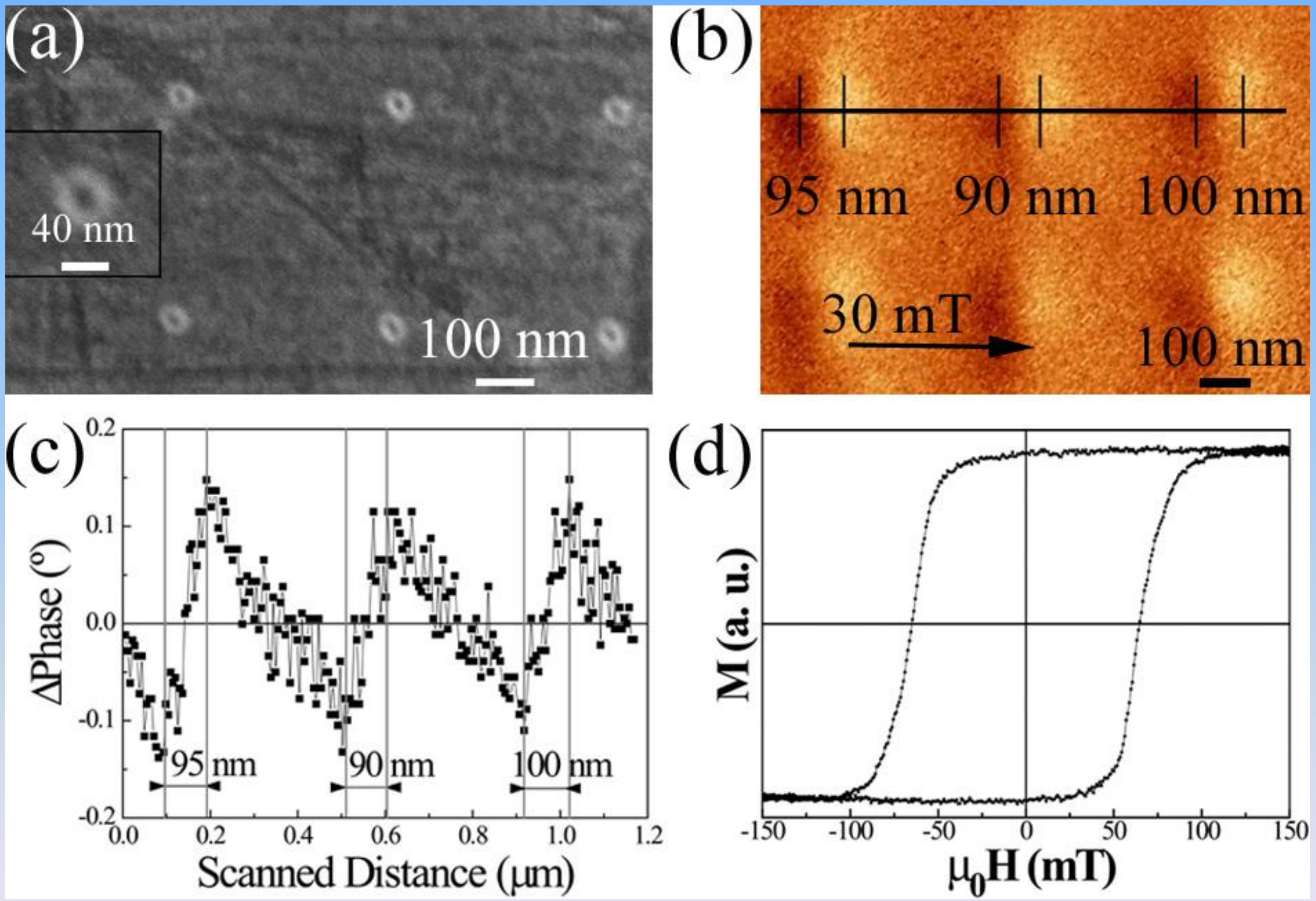


•Square-shaped loops and coercivity enhancement

(typical of single domain states)

# 4. Results and Discussion: Fe-based metallic glass

# 4. Results and Discussion: Fe-based metallic glass

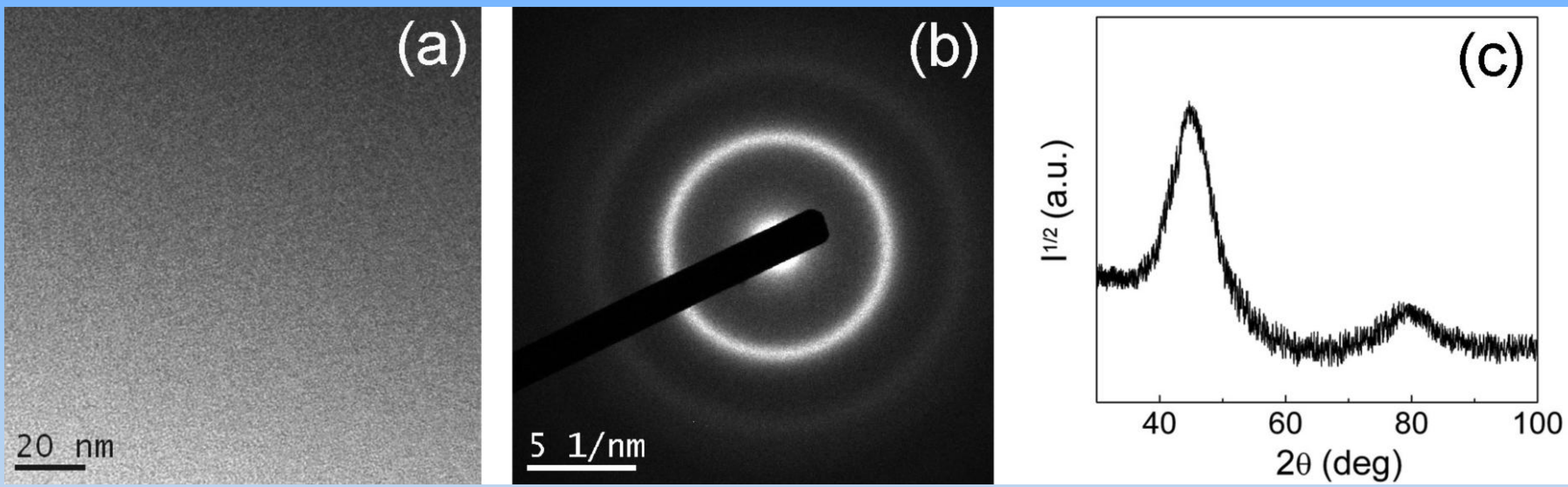


Transmission electron microscope (TEM) image (with the corresponding SAED pattern) and XRD pattern reveal the amorphous nature of the as-cast sample.

$Fe_{67.7}B_{20}Cr_{12}Nb_{0.3}$

# 4. Results and Discussion: Fe-based metallic glass

Thermal stability and magnetic transitions (DSC vs. TMG curves)

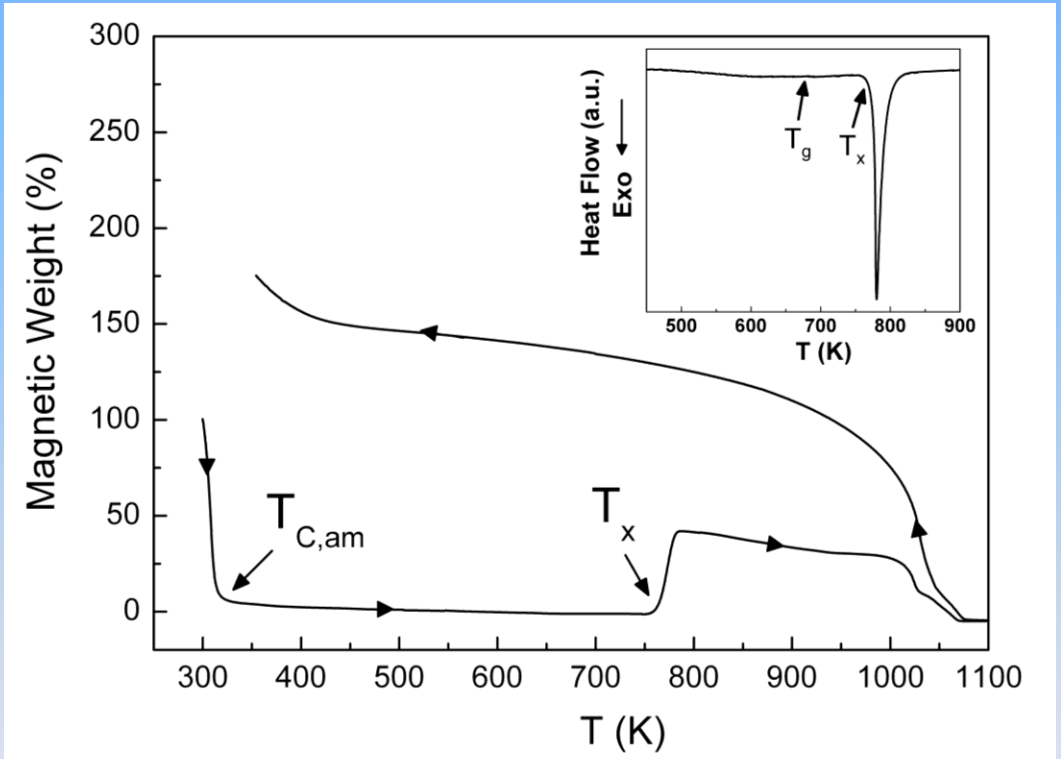


- Glass transition temperature: $T_g$ = 670 K
- Crystallization temperature: $T_x$ = 780 K
- Large supercooled liquid region ($\Delta T$) = 110 K
- Curie temperatures of the crystalline phases beyond 1000 K

# 4. Results and Discussion: Fe-based metallic glass

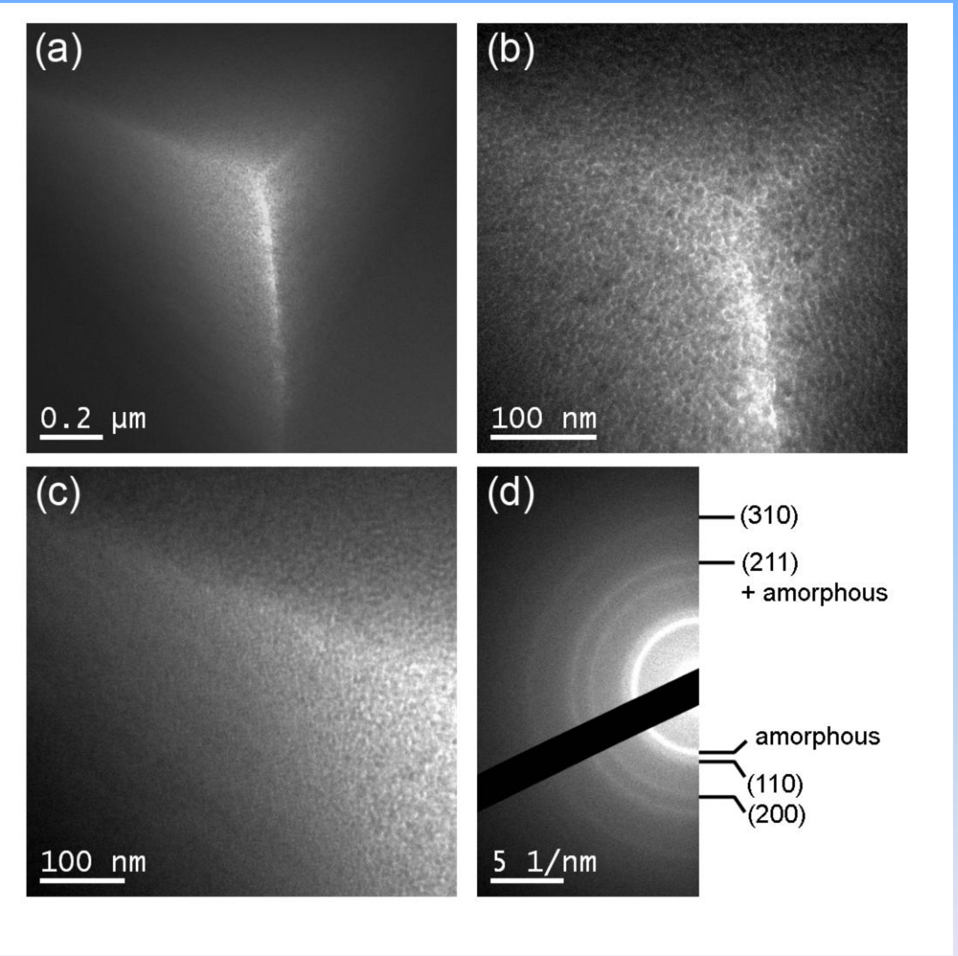


- Nanoindentation induces crystallization of α-Fe.

- Progressive decrease of the crystallite size towards the edge of the indents (crystallite size around 8 nm at the central part of the indents).

$P_{max}$ = 20 mN

# 4. Results and Discussion: Fe-based metallic glass

- Polar hysteresis loops at room temperature and above $T_{C,am}$ = 330 K

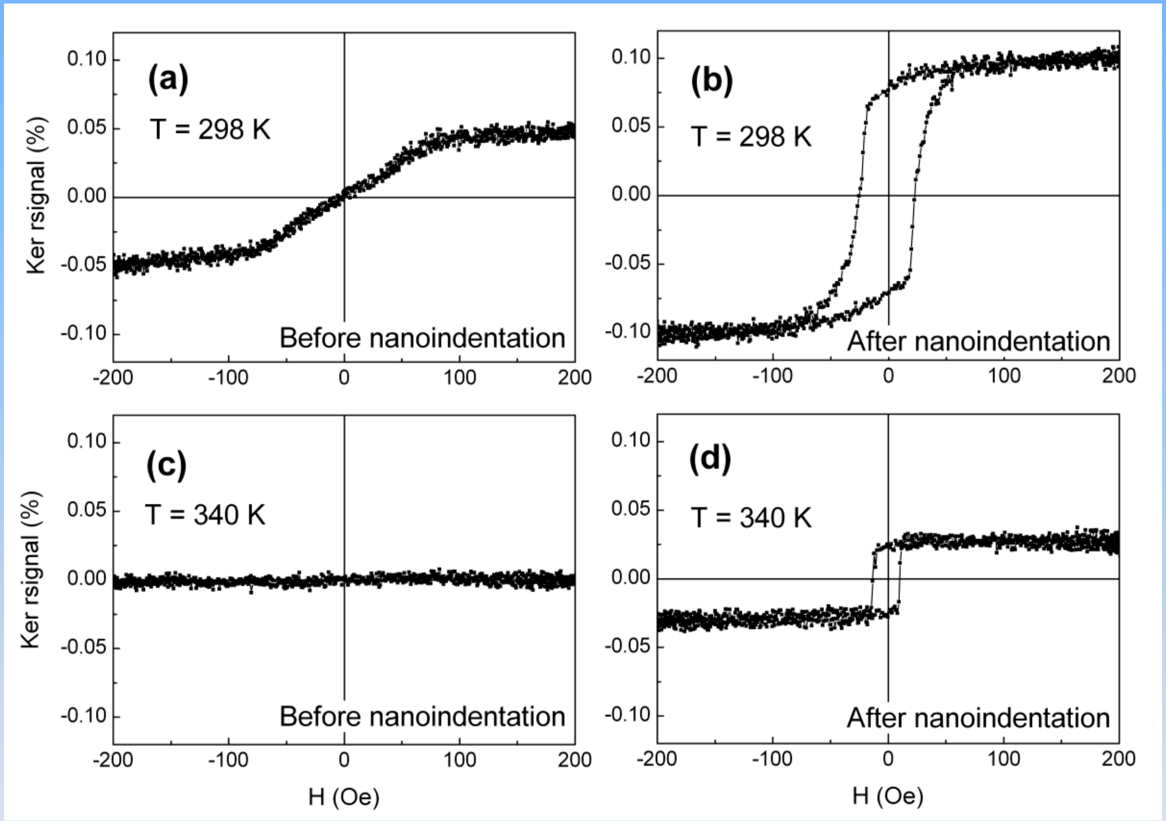


- **At T = 298 K:**

- *In-plane* magnetic anisotropy before indentation

- *Perpendicular-to-plane* magnetic anisotropy after indentation

- **At T = 340 K:**

- *No ferromagnetism* before indentation

- *Perpendicular-to-plane* magnetic anisotropy after indentation

- The Kerr signal increases in the indented regions.

# 4. Results and Discussion: Fe-based metallic glass

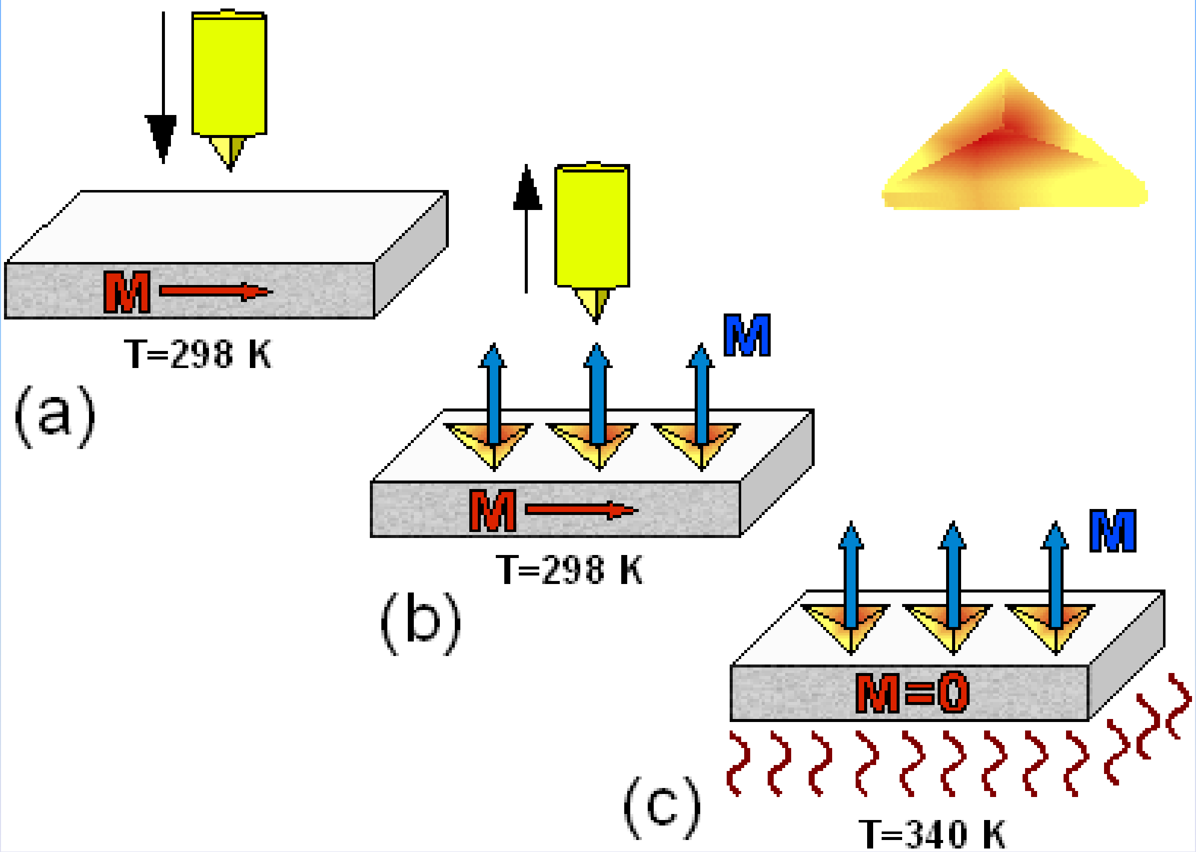


- **At T = 298 K:**

- *In-plane* magnetic anisotropy before indentation

- *Perpendicular-to-plane* magnetic anisotropy after indentation

- **At T = 340 K:**

- *No ferromagnetism* before indentation

- *Perpendicular-to-plane* magnetic anisotropy after indentation

# 4. Results and Discussion: Fe-based metallic glass

**Atomic force microscopy**

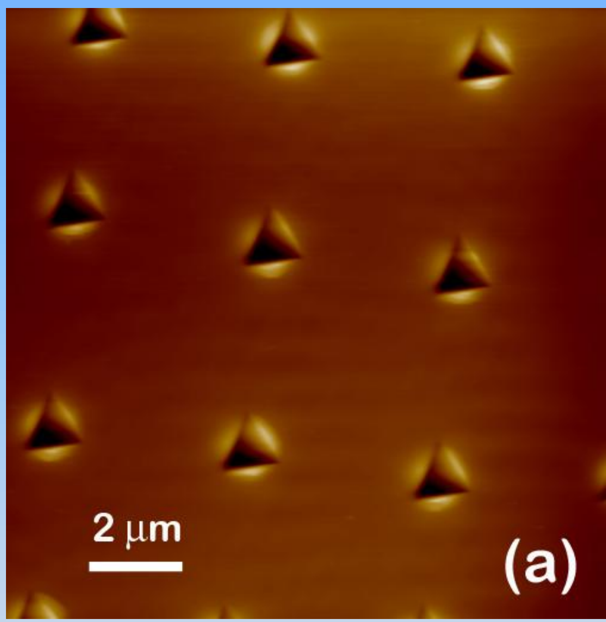


**Magnetic force microscopy**

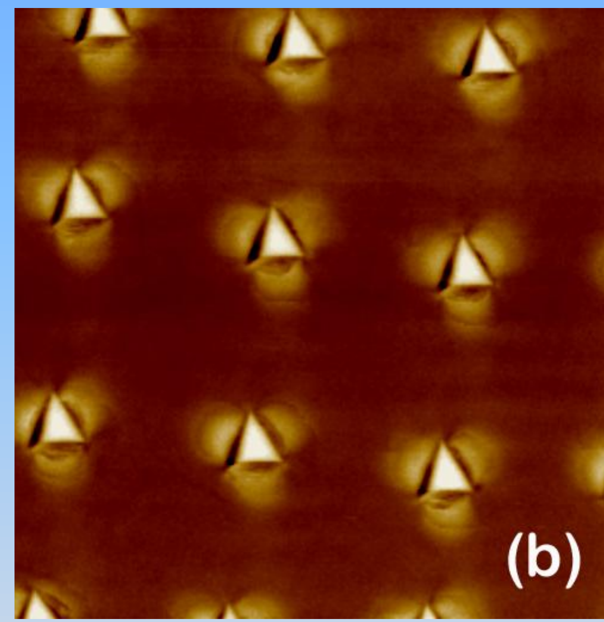


- Magnetic contrast expands towards the pile-up region.
- No magnetic domains around the indentations because the initial amorphous ribbon is very soft (i.e., with large domain sizes).

# 4. Results and Discussion: Fe-based metallic glass

- Polar hysteresis loops at room temperature and above $T_{C,am}$ = 330 K

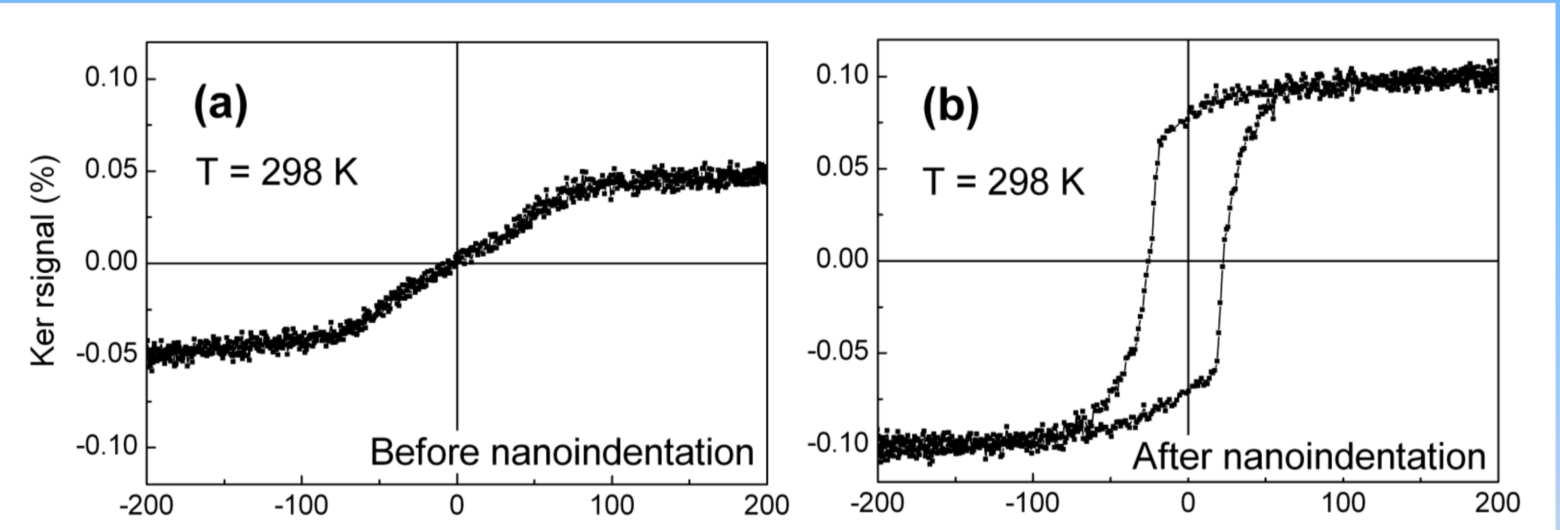


- Why does the Kerr signal increases in the indented regions ?
- Why does the remanence-to-saturation ratio increases in the indented regions ?

# 4. Results and Discussion: Fe-based metallic glass

- The increase of saturation magnetization after indentation is due to nanocrystallization: $M_{S,am}$ = 45 emu/g ; $M_{S,\alpha\text{-Fe}}$ = 217 emu/g
- The reorientation transition (from in-plane to perpendicular-to-plane) is ascribed to the inverse magnetostriction (or Villari) effect:

$$E_{magneto-elastic} = -\frac{3}{2}\lambda\sigma\cos^2(\theta)$$

$\lambda$: material-dependent magnetostriction constant
$\sigma$: stress (compressive, i.e. negative)
$\theta$: angle between the saturation magnetization and $\sigma$ direction

- Since $\lambda_{\alpha\text{-}Fe,\text{poly}}$ = -6.8 x $10^{-6}$ erg/cc, the product $\lambda \cdot \sigma$ is positive; therefore:

$E_{magneto-elastic}$ is minimized for $\theta$ = 0º or 180º. This means *M* will tend to orient parallel / antiparallel to the compressive indentation stress, i.e., mainly perpendicular-to-plane.

# 4. Results and Discussion: Fe-based metallic glass

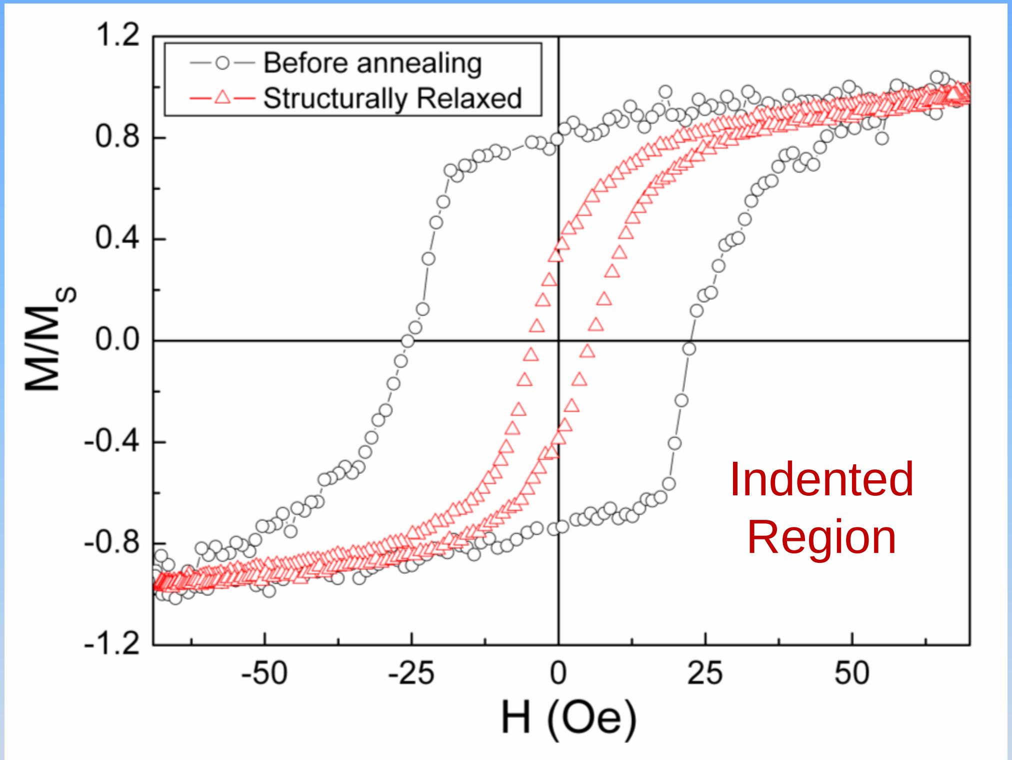


Hysteresis loops, measured by polar MOKE, at room temperature.

Annealing at 530 K for 30 min releases strains (structural relaxation)

The remanence-to-saturation ratio is reduced.

# 4. Results and Discussion: Fe-based metallic glass

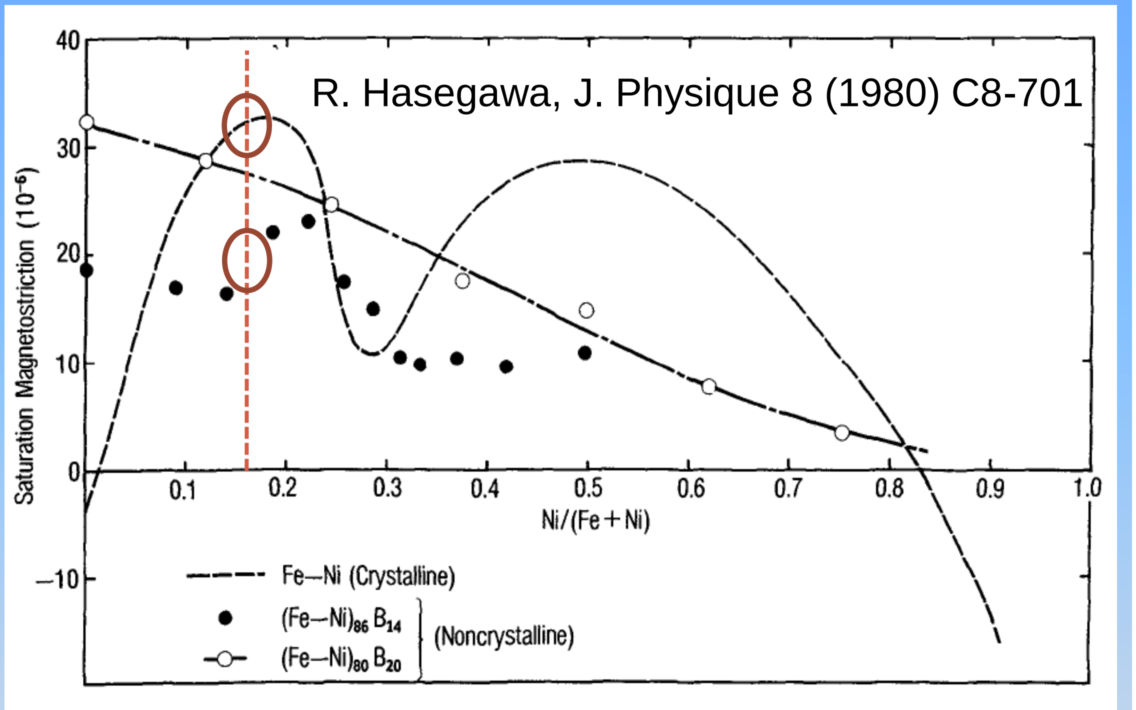


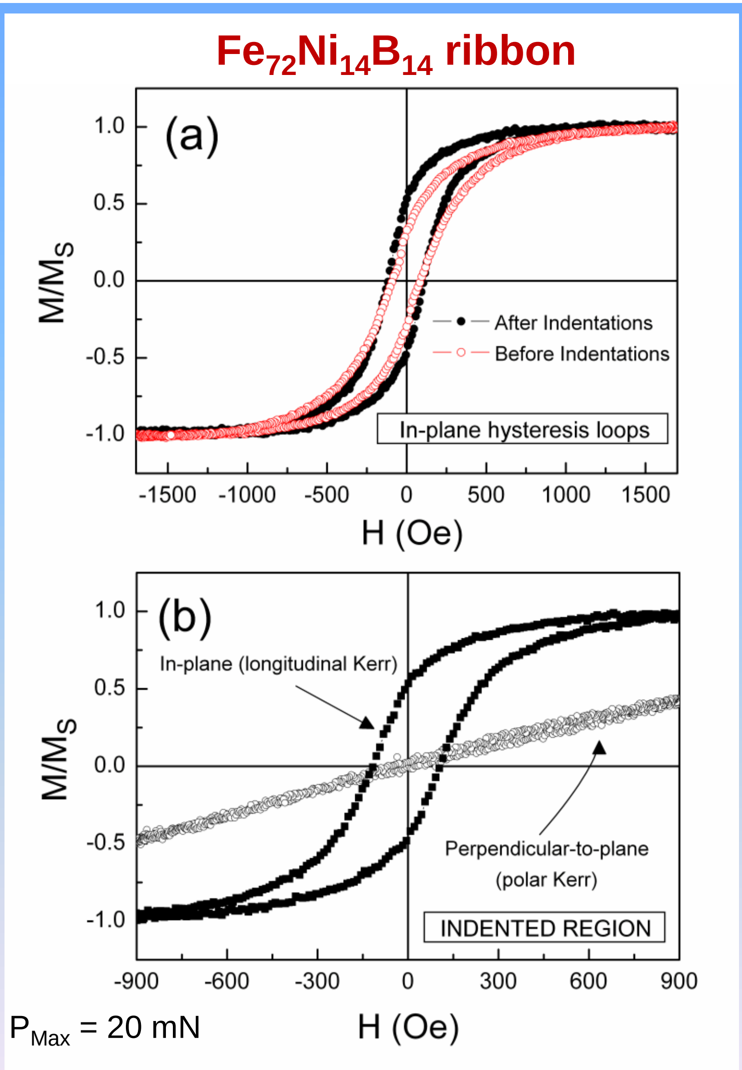


- Positive magnetostriction constants both in the amorphous and crystalline states.
- No deformation-induced reorientation towards out-of-plane anisotropy.

# 5. Conclusions

- In certain materials, magnetic patterning can be induced by nanoindentation and ion irradiation.

  - ➢ In $Fe_{60}Al_{40}$, ion irradiation causes appearance of confined ferromagnetism with minimum surface modification. Appropriate heating removes the induced ferromagnetism.

  - ➢ In Fe-based glass, nanoindentation causes local changes in the magnetic properties.

    - ❖ Perpendicular orientation only for crystallized regions with negative magnetostriction constant.

# References and Acknowledgements

- **Related articles:**


- J. Fassbender et al., *Phys. Rev. B* 77 (2008) 174430.
- E. Menéndez et al., *Small* 5 (2009) 229-234.
- J. Sort et al., *Small* 6 (2010) 1543-1549.
- A. Varea et al., *J. Appl. Phys.* 109 (2011) 093918.
- E. Menéndez et al. *Revista de Física* (2012, in press).


- **Acknowledgements**

Financial support from the 2005SGR-00401, 2009SGR-1292, PNL2006-019 and the MAT-2007-61629 research projects